

1 **Supplement to: A Conceptual Model of Polar Overturning Circulations**

2 Thomas W. N. Haine*

3 *Earth & Planetary Sciences, Johns Hopkins University, Baltimore, Maryland*

4 *Corresponding author: Thomas W. N. Haine, Thomas.Haine@jhu.edu

ABSTRACT

5 Supplementary material on theory and numerical methods.

6 S1. Model Solution

7 Adding the mass, salt, and heat equations together yields (from (12) and moving the known
8 parameters to the right hand side):

$$\begin{pmatrix} \rho_2 & \rho_3 & \rho_i \\ \rho_2 S_2 & \rho_3 S_3 & \rho_i S_i \\ c_p \rho_2 T_f & c_p \rho_3 T_3 & -\rho_i L' \end{pmatrix} \begin{pmatrix} U_2 \\ U_3 \\ U_i \end{pmatrix} = \begin{pmatrix} \mathcal{F} - \rho_1 U_1 \\ -\rho_1 U_1 S_1 \\ \mathcal{Q} - c_p \rho_1 U_1 T_1 \end{pmatrix}. \quad (\text{S1})$$

9 This system is three equations in five unknowns $\{U_2, U_3, U_i, T_3, S_3\}$. The five independent parameters
10 are $\{\mathcal{F}, \mathcal{Q}, U_1, U_1 T_1, U_1 S_1\}$. However, the entrainment model specifies T_3 as a function of Φ only
11 from (18) (as T_a is known from (13)). The entrainment model also specifies S_3 as a function of Φ
12 and S_s from (19). And (16), (17) and (19), (21) boil down to two more (nonlinear) equations for Φ
13 and S_s in terms of U_3 and S_3 . The system is therefore closed. It is solved as follows:

- 14 1. Select trial values for Φ and $S_s \leq S_s^{\max}$, and compute T_3, S_3 from (18) and (19).
- 15 2. Compute ρ_s and ρ_3 from (16) and (20) using the Gibbs Seawater (GSW) Oceanographic
16 Toolbox (IOC, SCOR, and IAPSO 2010). Skip statically unstable cases from (26).
- 17 3. Solve (S1) for $\{U_2, U_3, U_i\}$, and only retain solutions that satisfy the sign constraints (23) and
18 (24).
- 19 4. Compare the trial Φ with the theoretical value from (17) and (21), and only retain good fits
20 (within a threshold $\delta\Phi$).

21 These steps produce sets of candidate $\{U_2, U_3, U_i, S_s\}$ solutions that satisfy the entrainment model
22 within $\delta\Phi$. For fixed parameters $\{\mathcal{F}, \mathcal{Q}, U_1, U_1 T_1, U_1 S_1\}$ there may be zero or many solutions. If
23 there are many solutions, they sample the continuum of solutions that exist due to continuous
24 variations of Φ and S_s (which is discretely sampled in step 1).

25 For these candidate solutions to be valid, they must also satisfy the shelf system of equations.

26 From (12) they read:

$$\begin{pmatrix} \rho_1 & \rho_i \\ \rho_1 S_1 & \rho_i S_i \\ c_p \rho_1 T_1 & -\rho_i L' \end{pmatrix} \begin{pmatrix} u_1 \\ u_i \end{pmatrix} = \begin{pmatrix} \mathcal{F}_s - \rho_s u_s \\ -\rho_s u_s S_s \\ \mathcal{Q}_s - c_p \rho_s u_s T_f \end{pmatrix}. \quad (\text{S2})$$

27 Given a candidate u_s solution from (21), this is an overdetermined linear system for two variables
 28 $\{u_1, u_i\}$ with three equations. In addition the constraints $u_1 > 0$ and $u_i < U_i$ apply from (23). We
 29 seek $0 \leq \mathcal{Q}_s \leq \mathcal{Q}$ and $\mathcal{F} \leq \mathcal{F}_s \leq 0$ values that satisfy this problem. There may be zero, one, or a
 30 one-parameter infinity of solutions (where \mathcal{Q}_s and \mathcal{F}_s tradeoff).

31 This system is solved in two further steps. For each candidate $\{U_2, U_3, U_i, S_s\}$ solution:

32 5. Write one constraint on $\{\mathcal{Q}_s, \mathcal{F}_s\}$ by requiring that the right hand side of (S2) lies in the range
 33 of the matrix

$$\mathbf{E}_s = \begin{pmatrix} \rho_1 & \rho_i \\ \rho_1 S_1 & \rho_i S_i \\ c_p \rho_1 T_1 & -\rho_i L' \end{pmatrix}. \quad (\text{S3})$$

34 Call the range vector associated with the singular value of this matrix $\mathbf{s} = (s_1, s_2, s_3)^T$, which
 35 depends on the parameters in \mathbf{E}_s . Therefore,

$$s_1 (\mathcal{F}_s - \rho_s u_s) - s_2 \rho_s u_s S_s + s_3 (\mathcal{Q}_s - c_p \rho_s u_s T_f) = 0, \quad (\text{S4})$$

36 which is a linear relationship between \mathcal{Q}_s and \mathcal{F}_s . Consider it in the form

$$\mathcal{F}_s = \frac{\rho_s u_s}{s_1} \begin{pmatrix} 1 & S_s & T_f \end{pmatrix} \mathbf{s} - \frac{s_3}{s_1} \mathcal{Q}_s, \quad (\text{S5})$$

37 where

$$\frac{s_3}{s_1} = \frac{S_1 - S_i}{L' S_1 + c_p T_1 S_i} \quad (\text{S6})$$

38 is positive so that increasing positive Q_s means increasing negative \mathcal{F}_s . We require $0 \leq Q_s \leq Q$
 39 and $\mathcal{F} \leq \mathcal{F}_s \leq 0$. To test these inequalities, compute the $\mathcal{F}_s(Q_s)$ values from (S5) at the
 40 $Q_s \in \{0, Q\}$ limits. This allows calculation of the $\{\mathcal{F}_s, Q_s\}$ pairs, call them $\{\mathcal{F}_s^a, Q_s^a\}$, that
 41 bound the line segment of acceptable values, if they exist.

42 6. If they do exist, compute the corresponding $\{u_1, u_i\}$ solutions from

$$\begin{pmatrix} u_1 \\ u_i \end{pmatrix} = (\mathbf{E}_s^T \mathbf{E}_s)^{-1} \mathbf{E}_s^T \begin{pmatrix} \mathcal{F}_s^a - \rho_s u_s \\ -\rho_s u_s S_s \\ Q_s^a - c_p \rho_s u_s T_f \end{pmatrix}. \quad (\text{S7})$$

43 The line segment $\{\mathcal{F}_s^a, Q_s^a\}$ maps to a line segment in $\{u_1, u_i\}$ space. Finally, the inequalities
 44 on $\{u_1, u_i\}$ from (23) and (25) must be satisfied. Again, that yields, in general, zero, one, or an
 45 infinite number of $\{Q_s, \mathcal{F}_s\}$ pairs that qualify. Corresponding to every valid $\{Q_s, \mathcal{F}_s\}$ pair is a
 46 unique $\{u_1, u_i\}$ pair. If there is an infinite number, then it is a one parameter infinity.

47 This strategy finds solutions that exactly satisfy the conservation equations and inequalities, but
 48 that approximate the entrainment parameterization formula (17), within threshold $\delta\Phi$. For each
 49 set of parameter values, there are zero, one, or many valid solutions for $\{U_2, U_3, U_i, S_s\}$. For each
 50 one of these solutions, there are zero, one, or an infinite number of $\{u_1, u_i\}$ solutions.

51 **S2. Theory for tradeoff between entrainment and shelf circulation**

52 The entrainment/shelf salinity tradeoff is described as follows (from (17) and (21)):

$$\begin{aligned} \Phi &= 1 - \gamma \frac{|u_s|^{1/3}}{(\rho_s - \rho_a)^{2/3}}, \\ U_3 &= \frac{u_s}{1 - \Phi}. \end{aligned} \quad (\text{S8})$$

53 Now $\rho_s - \rho_a \approx \rho_0 \beta \Delta S_s$, where $\Delta S_s = S_s - S_a^*$, where S_a^* is the salinity of the water at the freezing
 54 temperature with the same density as the aW: $\rho_a = \rho(T_f, S_a^*)$. So for fixed U_3 (which is an

55 approximation; see below):

$$\Phi = 1 - \frac{\gamma^{3/2}}{\rho_0 \beta \Delta S_s} |U_3|^{1/2}, \quad (\text{S9})$$

56 which is (28). In practice, U_3 varies a little from this theoretical curve because S_3 and T_3 depend
57 on Φ and S_s too. Fig. 7 shows this variation is relatively weak.

58 S3. Theoretical arguments for degeneracy of forcing parameters

59 Here we justify the statement that acceptable model solutions for U_2 (for example) in the space of
60 flux parameters, $\{\mathcal{F}, Q, U_1, U_1 T_1, U_1 S_1\}$ (for fixed ϕ), typically lie along the line $Q + L\mathcal{F} - \rho_0 c_p U_1 T_1$.
61 This degeneracy is a great simplification because it points to the importance of a single compound
62 parameter, rather than the full five dimensional parameter space. It thereby provides insight into
63 the dominant processes in the model. Two lines of reasoning are shown:

64 First, consider the following approximation: The seawater freezing temperature, sea ice temper-
65 ature, and sea ice salinity are zero $T_f = T_i = S_i = 0$ (which implies that $L' = L$) and the densities are
66 identical $\rho_1 = \rho_2 = \rho_3 = \rho_i = \rho_0$. The equations for the system (S1) as a whole now read:

$$\begin{pmatrix} 1 & 1 & 1 \\ S_2 & S_3 & 0 \\ 0 & 0 & -L \end{pmatrix} \begin{pmatrix} U_2 \\ U_3 \\ U_i \end{pmatrix} \approx \begin{pmatrix} \mathcal{F}/\rho_0 - U_1 \\ -U_1 S_1 \\ Q/\rho_0 - c_p U_1 T_1 \end{pmatrix}. \quad (\text{S10})$$

67 In the final equation assume that $|c_p U_3 T_3| \ll |L U_i|$ too. This approximation is not wholly supported
68 by the heat budgets shown in Figs. 4 and 5, although the AW term is smaller than the sea ice term
69 in both cases (see below). Physically, the approximation means that the freezing rate to form sea
70 ice U_i is proportional to the difference between ocean heat loss Q and AW heat flux $c_p \rho_0 U_1 T_1$. It
71 is important because it reduces the rank of (S10) by one. Therefore, $U_i \approx (Q - c_p \rho_0 U_1 T_1) / (\rho_0 L)$

72 and

$$\begin{pmatrix} 1 & 1 \\ S_2 & S_3 \end{pmatrix} \begin{pmatrix} U_2 \\ U_3 \end{pmatrix} \approx \begin{pmatrix} \mathcal{F}/\rho_0 - U_1 + \mathcal{Q}/(\rho_0 L) - c_p U_1 T_1/L \\ -\rho_0 U_1 S_1 \end{pmatrix}. \quad (\text{S11})$$

73 The volume budget therefore reads

$$U_1 + U_2 + U_3 \approx \mathcal{F}/\rho_0 + \mathcal{Q}/(\rho_0 L) - c_p U_1 T_1/L \quad (\text{S12})$$

74 The inverse of the matrix in (S11) is

$$\frac{1}{S_3 - S_2} \begin{pmatrix} S_3 & -1 \\ -S_2 & 1 \end{pmatrix} \quad (\text{S13})$$

75 and therefore the OW flux U_2 is

$$U_2 \approx \frac{[\mathcal{Q} + L\mathcal{F} - \rho_0 c_p U_1 T_1] + \rho_0 L (S_1/S_3 - 1) U_1}{\rho_0 L (1 - S_2/S_3)}. \quad (\text{S14})$$

76 The second numerator term, which is proportional to $(S_1/S_3 - 1) U_1$, is smaller in practice than the
 77 first term in brackets, which dominates the numerator. Therefore, this formula says that the OW
 78 flux U_2 is essentially proportional to $\mathcal{Q} + L\mathcal{F} - \rho_0 c_p U_1 T_1$.

79 Second, the exact formula for $U_2 \equiv \mathcal{N}/\mathcal{D}$ is

$$U_2 = \frac{(1 - S_i/S_3) \mathcal{Q} + (L' + c_p T_3 S_i/S_3) \mathcal{F} + L' \rho_1 (S_1/S_3 - 1) U_1 + c_p \rho_1 [(S_1/S_3 - S_i/S_3) T_3 + (S_i/S_3 - 1) T_1] U_1}{\rho_2 \{L' (1 - S_2/S_3) + c_p [(S_i/S_3 - S_2/S_3) T_3 + (1 - S_i/S_3) T_f]\}} \quad (\text{S15})$$

80 which results from solving (S1). Notice that the flux parameters appear exclusively in the numerator
 81 \mathcal{N} as a linear combination of $\mathcal{F}, \mathcal{Q}, U_1, U_1 T_1$ and $U_1 S_1$, from the right hand side of (S1). This
 82 property depends on the matrix form of the equations. Vanishing of U_2 (loss of the estuarine cell)
 83 is therefore controlled by \mathcal{N} vanishing. The coefficients in \mathcal{N} depend on T_3, S_3 , however, which
 84 vary, and the denominator \mathcal{D} also depends on them. This is the reason that solving exactly for U_2
 85 is hard (sections S1 and S5). Now consider what can be said about \mathcal{N} and U_2 without knowing T_3

86 and S_3 : Approximate S_3 with S_1 and drop the uncertain T_3 terms to give:

$$\begin{aligned}
\mathcal{N} &\approx \mathcal{N}^* \equiv (1 - S_i/S_1) \mathcal{Q} + L' \mathcal{F} + \rho_1 c_p (S_i/S_1 - 1) T_1 U_1, \\
&\approx \mathcal{Q} + L \mathcal{F} - \rho_0 c_p U_1 T_1, \\
&\approx \rho_i L' U_1 (1 + U_2/U_1 + U_3/U_1),
\end{aligned} \tag{S16}$$

87 which is (29)–(31). Plotting the distribution of U_2 against \mathcal{N}^* for various forcing parameters tests
88 these assumptions by quantifying what can be said about U_2 without knowing T_3 and S_3 , as in
89 Fig. 8.

90 **S4. Theory for parametric locations of PW crises and OW emergency**

91 Consider first the edge of the salt crisis hatched region in Fig. 6 near experiment 2, indicating
92 $U_2 = 0$. From (S15) that \mathcal{Q} limit, \mathcal{Q}^+ , is

$$\mathcal{Q}^+ = \max \left\{ \frac{\left((L' + c_p T_3 S_i/S_3) \mathcal{F} + L' \rho_1 (S_1/S_3 - 1) U_1 + c_p \rho_1 [(S_1/S_3 - S_i/S_3) T_3 + (S_i/S_3 - 1) T_1] U_1 \right)}{S_i/S_3 - 1} \right\}, \tag{S17}$$

93 which is controlled by the variation of T_3, S_3 . For the salt crisis, $T_3 = T_f$ and $S_3 = S_s^-$, where S_s^- is the
94 shelf salinity for vanishing entrainment $\Phi = 0$, given implicitly by $\rho(T_f, S_s^-) = |U_1|^{1/2} \gamma^{3/2} + \rho(T_a, S_a)$
95 from (17), (21), and $U_2 = 0$. Therefore,

$$\mathcal{Q}^+ = \frac{\left(L' S_s^- + c_p T_f S_i \right) (\rho_1 U_1 - \mathcal{F}) - \rho_1 \left(L' + c_p T_f \right) U_1 S_1}{S_s^- - S_i} + c_p \rho_1 U_1 T_1. \tag{S18}$$

96 All the terms in this expression can be computed with knowledge of the system parameters. See
97 Fig. 9.

98 Consider next the parametric location of the OW emergency in Fig. 6, given by \mathcal{Q}^* , for which
99 $U_3 = 0$. By solving (S1) for $U_3 = 0$:

$$\mathcal{Q}^* = \frac{\left(L' S_2 + c_p T_f S_i \right) (\rho_1 U_1 - \mathcal{F}) - \rho_1 \left(L' + c_p T_f \right) U_1 S_1}{S_2 - S_i} + c_p \rho_1 U_1 T_1. \tag{S19}$$

100 Notice the similarity with (S18) and that all these terms can be computed with knowledge of the
 101 system parameters. See Fig. 9.

102 Consider finally the edge of the heat crisis in Fig. 6, similar to experiment 1, given by Q^- . Like
 103 the salt crisis

$$Q^- = \frac{(L'S_3 + c_p T_3 S_i)(\rho_1 U_1 - \mathcal{F}) - \rho_1 (L' + c_p T_3) U_1 S_1}{S_3 - S_i} + c_p \rho_1 U_1 T_1. \quad (\text{S20})$$

104 Predicting the values of T_3 and S_3 without solving the model is tricky, however. Fig. 9 shows three
 105 hierarchical approaches to estimate T_3 and S_3 : (i) The patch shows upper and lower bounds for
 106 Q^- (plotted using the related \mathcal{N}^* parameter in Fig. 9). These bounds derive from the range of
 107 possible (T_3, S_3) values for which the OW density equals the AW density. Furthermore, the Q^-
 108 upper bound cannot exceed the Q^* value associated with the OW emergency (because the OW
 109 emergency and the heat crisis exclude one another). These criteria guarantee static stability of AW
 110 and OW, regardless of the details of the entrainment process or the shelf water properties. In this
 111 sense, they make minimal assumptions. (ii) The group of points labelled “ Q^- heat crisis mid 2”
 112 use (T_3, S_3) values that assume $\rho(T_3 = T_a, S_3) = \rho(T_1, S_1)$. The assumption $T_3 = T_a$ corresponds to
 113 no upper limit on S_s or therefore on ρ_s . (iii) The group of points labelled “ Q^- heat crisis mid 1”
 114 estimates the maximum entrainment with

$$\Phi_{\max} \approx 1 - \frac{\gamma^{3/2} |U_1|^{1/2}}{\rho(T_f, S_s^{\max}) - \rho_a}, \quad (\text{S21})$$

115 from (17) assuming that $u_s \approx U_3 \approx -U_1$. Given Φ_{\max} , T_3 and S_3 follow from (18) and (19).

116 **S5. Theory for selection of OW properties T_3, S_3 from budget equations**

117 The OW properties T_3, S_3 are essential for understanding solutions to the model, and specifically
 118 the controls on the strength of the estuarine cell U_2 . Here we extend sections S3 and S4 to discuss

119 how these properties are selected, in particular, how the basin-wide budget (S1) interacts with the
 120 sign constraints on the volume fluxes (23) and (24).

121 Consider again the formula for $U_2 = \mathcal{N}/\mathcal{D}$ (S15):

$$\begin{aligned} S_3 \mathcal{N} &= (S_3 - S_i) \mathcal{Q} + (L' S_3 + c_p T_3 S_i) \mathcal{F} + L' \rho_1 (S_1 - S_3) U_1 + c_p \rho_1 [(S_1 - S_i) T_3 + (S_i - S_3) T_1] U_1, \\ \frac{S_3}{\rho_2} \mathcal{D} &= L' (S_3 - S_2) + c_p [(S_i - S_2) T_3 + (S_3 - S_i) T_f]. \end{aligned} \quad (\text{S22})$$

122 Both the numerator \mathcal{N} and denominator \mathcal{D} depend on T_3 and S_3 , as previously discussed. Therefore,
 123 consider the functions $\mathcal{N}(T_3, S_3)$ and $\mathcal{D}(T_3, S_3)$ in the temperature/salinity (TS) plane. We know
 124 that $-U_1 \lesssim U_2 < 0$ for valid solutions, so the signs of \mathcal{N} and \mathcal{D} must be different and \mathcal{D} cannot
 125 be very small. Valid T_3, S_3 points are therefore constrained by the $\mathcal{N}(T_3, S_3) = 0$ and $\mathcal{D}(T_3, S_3) = 0$
 126 contours because $\mathcal{N}(T_3, S_3) = 0$ defines the locus of $U_2 = 0$ points and $\mathcal{D}(T_3, S_3) = 0$ defines the
 127 locus of $|U_2| = \infty$ points in TS space. What are these loci of points? For $\mathcal{N}(T_3, S_3) = 0$,

$$T_3 = \frac{\mathcal{Q} S_i - \rho_1 (L' S_1 + c_p S_i T_1) U_1 + S_3 [\rho_1 U_1 (L' + c_p T_1) - \mathcal{Q} - L' \mathcal{F}]}{c_p [\mathcal{F} S_i + \rho_1 (S_1 - S_i) U_1]}, \quad (\text{S23})$$

128 which is a line. The line intercepts the freezing temperature at salinity S^*

$$S^* = \frac{c_p T_f [\mathcal{F} S_i + \rho_1 (S_1 - S_i) U_1] + \rho_1 (L' S_1 + c_p S_i T_1) U_1 - \mathcal{Q} S_i}{\rho_1 U_1 (L' + c_p T_1) - \mathcal{Q} - L' \mathcal{F}}, \quad (\text{S24})$$

129 and has slope

$$\frac{\rho_1 U_1 (L' + c_p T_1) - \mathcal{Q} - L' \mathcal{F}}{c_p [\mathcal{F} S_i + \rho_1 (S_1 - S_i) U_1]} \approx \frac{L}{c_p S_1}. \quad (\text{S25})$$

130 This line is entirely determined by the flux parameters $\{\mathcal{Q}, \mathcal{F}, U_1, T_1 U_1, S_1 U_1\}$ and constants. Think
 131 of it as having (nearly) fixed slope and an intercept S^* that changes with the flux parameters: it
 132 slides left and right in TS space, for instance as \mathcal{Q} decreases and increases. Figure S1 illustrates
 133 this behaviour. For $\mathcal{D}(T_3, S_3) = 0$,

$$T_3 = \frac{-L' S_2 - c_p T_f S_i + S_3 (L' + c_p T_f)}{c_p (S_2 - S_i)}, \quad (\text{S26})$$

134 which again is a line. The line intercepts the freezing temperature at salinity S_2 and has slope

$$\frac{L' + c_p T_f}{c_p (S_2 - S_i)} \approx \frac{L}{c_p S_2}. \quad (\text{S27})$$

135 This line is entirely determined by S_2 and constants. Think of it as being fixed to the PW properties
 136 (T_f, S_2) with (nearly) fixed positive slope (nearly) parallel to the $\mathcal{N} = 0$ line. For valid U_2 solutions,
 137 OW properties T_3 and S_3 cannot lie in the TS gap between the $\mathcal{N} = 0$ and $\mathcal{D} = 0$ lines because in
 138 this gap the signs of \mathcal{N} and \mathcal{D} are the same and $U_2 \neq 0$. Also, as OW properties approach the
 139 $\mathcal{D} = 0$ line, for instance as $S^* \rightarrow S_2$, U_2 becomes very sensitive to small changes in T_3 and S_3 .

140 Consider also the formulae for U_3 and U_i from solving (S1):

$$-\frac{\rho_3 \mathcal{D}}{\rho_2} U_3 = (S_2 - S_i) \mathcal{Q} + (L' S_2 + c_p T_f S_i) \mathcal{F} + L' \rho_1 (S_1 - S_2) U_1 + c_p \rho_1 [(S_1 - S_i) T_f + (S_i - S_2) T_1] U_1 \quad (\text{S28})$$

$$-\frac{\rho_i \mathcal{D}}{\rho_2} U_i = (S_3 - S_2) \mathcal{Q} + c_p (T_3 S_2 - T_f S_3) \mathcal{F} - c_p T_f \rho_1 (S_1 - S_3) U_1 + c_p \rho_1 [(S_1 - S_2) T_3 + (S_2 - S_3) T_1] U_1. \quad (\text{S29})$$

141 Notice that the expression for U_3 resembles (S22) with S_3 replaced by S_2 and T_3 replaced by T_f
 142 in the numerator. This formula only depends on T_3 and S_3 via the denominator \mathcal{D} , unlike (S22).
 143 Similarly, the expression for U_i resembles (S22) with S_i replaced by S_2 and L' replaced by $-c_p T_f$
 144 in the numerator. The denominator \mathcal{D} is unchanged, however, because it is proportional to the
 145 determinant of the matrix \mathbf{E} in (S1):

$$|\mathbf{E}| = -\rho_1 \rho_3 S_3 \mathcal{D} = \rho_2 \rho_3 \rho_i \left\{ L' (S_2 - S_3) + c_p [(S_2 - S_i) T_3 + (S_i - S_3) T_f] \right\}. \quad (\text{S30})$$

146 Therefore, the arguments above about the $\mathcal{D} = 0$ line apply unchanged. The requirement that
 147 $U_i < 0$ implies the existence of a third line in the TS plane corresponding to the $\mathcal{N} = 0$ line (S23):

$$T_3 = \frac{\mathcal{Q} S_2 + c_p \rho_1 (T_f S_1 - S_2 T_1) U_1 + S_3 [c_p \rho_1 U_1 (T_1 - T_f) - \mathcal{Q} + c_p T_f \mathcal{F}]}{c_p [\mathcal{F} S_2 + \rho_1 (S_1 - S_2) U_1]} \quad (\text{S31})$$

148 (again, changing $S_i \rightarrow S_2$ and $L' \rightarrow -c_p T_f$). This line depends on the flux parameters and S_2 . Its
 149 slope can change sign, but it passes through the PW properties (T_f, S_2) , like the $\mathcal{D} = 0$ line. The
 150 requirement that $U_i < 0$ means that valid (T_3, S_3) points cannot lie between the $\mathcal{D} = 0$ and this
 151 second $\mathcal{N} = 0$ line. Thus, the joint requirements that $U_i < 0$ and $U_2 < 0$ require that (T_3, S_3) points
 152 cannot lie between the two $\mathcal{N} = 0$ lines defined by (S23) and (S31). (Because the $\mathcal{D} = 0$ line
 153 lies between the two $\mathcal{N} = 0$ lines.) Physically, this idea means that the OW temperature T_3 must
 154 be relatively close to the AW temperature or freezing, and not in between. The requirement that
 155 $U_3 < 0$ adds no new constraint because its numerator does not depend on (T_3, S_3) : It implies an
 156 inequality on S_2 , but this restriction is automatically satisfied.

157 These constraints combine with three other straightforward constraints to restrict possible OW
 158 properties, namely $\rho_3 \geq \rho_1$, and $T_f \leq T_3 \leq T_a$. They are shown schematically in Fig. S1. The
 159 intersection of all these restrictions are plotted as the brown patches in Figs. 3, 4, 5, and S1. In
 160 practice, the solutions lie close to the $\mathcal{N} = 0$ line given by (S23). Therefore, the selection of the
 161 strong (weak) shelf circulation mode with cold (warm) OW requires positive (negative) $S^* - S_2$.
 162 The additional requirement to satisfy the entrainment model (green patches, see section S6) selects
 163 a sub-region of these patches as valid solutions (plotted as the OW points in the solution figures).

164 **S6. Theory for selection of OW properties T_3, S_3 from entrainment model**

165 Consider T_3, S_3 constraints from the entrainment model. From (16)–(19) and (21),

$$\begin{aligned}
 1 - \Phi &= \frac{\gamma^{3/2} |U_3|^{1/2}}{\rho_s - \rho_a}, \\
 &= \frac{T_a - T_3}{T_a - T_f}, \\
 &= \frac{S_a - S_3}{S_a - S_s}.
 \end{aligned} \tag{S32}$$

166 Therefore,

$$\begin{aligned} T_3 &= T_a - (T_a - T_f) \frac{\gamma^{3/2} |U_3|^{1/2}}{\rho_s - \rho_a}, \\ S_3 &= S_a + (S_s - S_a) \frac{\gamma^{3/2} |U_3|^{1/2}}{\rho_s - \rho_a}. \end{aligned} \quad (\text{S33})$$

167 The common fraction is proportional to the departure in OW properties from aW properties.
168 Its maximum conceivable value is $\gamma^{3/2} |U_1|^{1/2} / (\rho_1 - \rho_a) = 1 - \Phi_{min}$, which is associated with the
169 minimum value of entrainment fraction Φ_{min} . This minimum entrainment value can be greater than
170 zero. Therefore, the lower limit for T_3 is $T_a - (T_a - T_f) (1 - \Phi_{min})$. For S_3 we seek the maximum
171 value of $(S_s - S_a) \gamma^{3/2} |U_3|^{1/2} / (\rho_s - \rho_a)$. An estimate of this maximum value is $\gamma^{3/2} |U_1|^{1/2} / \rho_0 \beta$,
172 because $\rho_s - \rho_a \approx \rho_0 \beta (S_s - S_a^*) > \rho_0 \beta (S_s - S_a)$ (from section S2, $\rho_a = \rho(T_f, S_a^*)$). Therefore,
173 the upper limit for S_3 is approximately $S_a + \gamma^{3/2} |U_1|^{1/2} / \rho_0 \beta$.

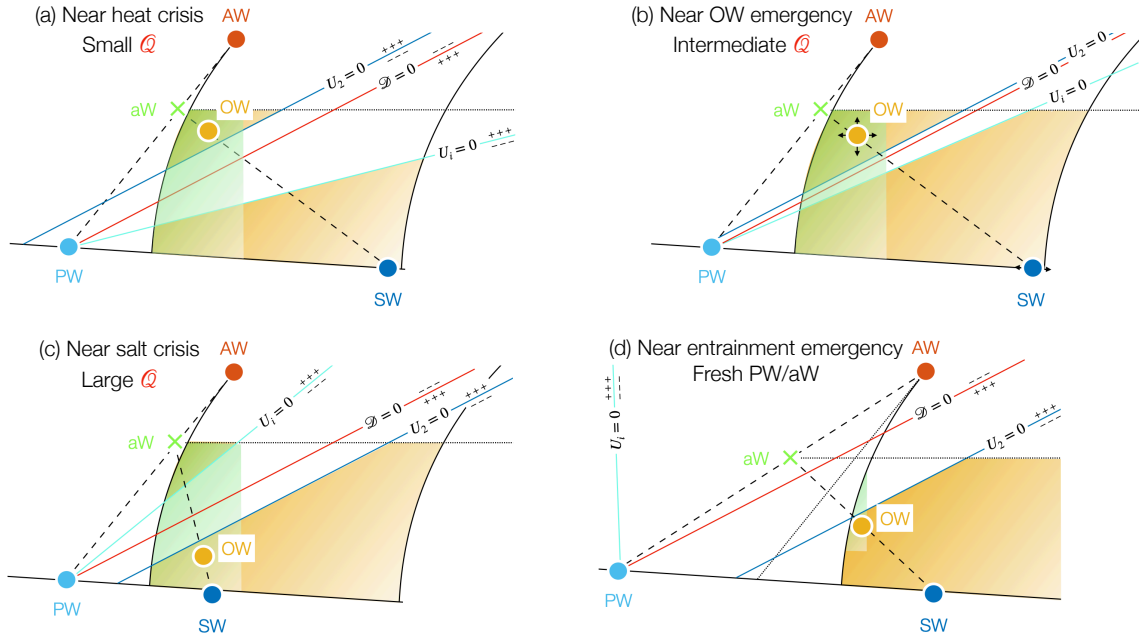
174 These limits on T_3 and S_3 are computed and plotted in Figs. 3, 4, and 5. For warmer/fresher aW,
175 the range of possible OW properties shrinks, because OW cannot be less dense than AW and also
176 because Φ_{min} decreases as ρ_a decreases. Note that the minimum value of Φ may not give a viable
177 solution if the budget equations (S1) cannot also be satisfied. In other words, Φ_{min} and the T_3, S_3
178 limits from (S33), are necessary, but not sufficient to specify the OW properties.

179 References

180 IOC, SCOR, and IAPSO, 2010: The international thermodynamic equation of seawater – 2010:
181 Calculation and use of thermodynamic properties. Tech. rep., Intergovernmental Oceanographic
182 Commission, Manuals and Guides No. 56, UNESCO (English). 196pp.

183 **LIST OF FIGURES**

184 **Fig. S1.** Schematic temperature salinity diagrams of the processes affecting OW properties for dif-
185 ferent limiting cases (see also Fig. 12). (a) Heat crisis, (b) OW emergency, (c) Salt crisis,
186 and (d) Entrainment emergency. The three lines are the contours of $U_2 = 0$ (blue), $U_i = 0$
187 (cyan), and denominator $\mathcal{D} = 0$ (red). Plus and minus signs indicate the signs either side
188 of these zero contours. The shaded brown patches show possible solutions that satisfy the
189 mass, freshwater, and heat budgets, plus the sign constraints on U_2, U_3 , and U_i . See Fig. 3
190 and section S5 for further explanation. The shaded green patches show possible solutions
191 that satisfy the entrainment model. See section S6 for further explanation. In practice, viable
192 solutions lie in the green and brown patches near the blue $U_2 = 0$ line. 15



193 FIG. S1. Schematic temperature salinity diagrams of the processes affecting OW properties for different limiting
 194 cases (see also Fig. 12). (a) Heat crisis, (b) OW emergency, (c) Salt crisis, and (d) Entrainment emergency. The
 195 three lines are the contours of $U_2 = 0$ (blue), $U_i = 0$ (cyan), and denominator $\mathcal{D} = 0$ (red). Plus and minus signs
 196 indicate the signs either side of these zero contours. The shaded brown patches show possible solutions that
 197 satisfy the mass, freshwater, and heat budgets, plus the sign constraints on U_2, U_3 , and U_i . See Fig. 3 and section
 198 S5 for further explanation. The shaded green patches show possible solutions that satisfy the entrainment model.
 199 See section S6 for further explanation. In practice, viable solutions lie in the green and brown patches near the
 200 blue $U_2 = 0$ line.